DOI: 10.63527/1607-8829-2026-1-5-16

V.A. Romaka[1] (https://orcid.org/0000-0002-2984-9513),
Yu.V. Stadnyk[2] (https://orcid.org/0000-0003-0692-2973),
L.P. Romaka[2] (https://orcid.org/0000-0001-5793-4435),
A.M. Horyn[2] (https://orcid.org/0000-0003-3483-8808),
A.V. Zelinskiy[2] (https://orcid.org/0000-0001-8473-1174),
V.Z. Pashkevych[1] (https://orcid.org/0000-0002-6849-652X)

[1]National University "Lvivska Politechnika",
12, S. Bandera str., Lviv, 79013, Ukraine;
[2]Ivan Franko National University of Lviv,
6, Kyryla and Mefodiya Str., Lviv, 79005, Ukraine

Corresponding author: V.A. Romaka, e-mail: *volodymyr.romaka@gmail.com*

Research on a New Semiconductor Thermoelectric Material n-$Zr_{1-x}Nb_xNiSn$. I. Experimental Results

The structural, electrokinetic, energetic, and magnetic properties of the new semiconductor thermoelectric material n-$Zr_{1-x}Nb_xNiSn$, $x = 0–0.07$, obtained by doping n-ZrNiSn with Nb atoms ($4d^45s^1$) by replacing Zr atoms ($4d^25s^2$) were investigated. The nature of the generated energy states and mechanisms of electrical conductivity were established. It was shown that in the n-$Zr_{1-x}Nb_xNiSn$ structure, there is a simultaneous substitution of Zr atoms by Nb atoms in different ratios, as well as the occupation of tetrahedral voids of the structure by Nb atoms. The decrease in the unit cell parameter $a(x)$ of n-$Zr_{1-x}Nb_xNiSn$ at concentrations $0 < x \leq 0.05$ is caused by the preferential partial substitution of Zr atoms ($r_{Zr} = 0.1602$ nm) by Nb atoms ($r_{Nb} = 0.1468$ nm), and the increase in the lattice parameter $a(x)$ at $x > 0.05$ is caused by the preferential occupation of tetrahedral voids of the structure by Nb atoms. Structural transformations of n-$Zr_{1-x}Nb_xNiSn$ generate two types of defects of donor nature and the corresponding energy states of the band gap ε_g, which meet the condition for obtaining the maximum efficiency of converting thermal energy into electrical energy. It is shown that the n-$Zr_{1-x}Nb_xNiSn$ semiconductor is a promising thermoelectric material.

Keywords: thermoelectric material, semiconductor, electronic structure, electrical resistivity, thermopower coefficient, thermoelectric figure of merit.

Citation: V.A. Romaka, Yu.V. Stadnyk, L.P. Romaka, A.M. Horyn, A.V. Zelinskiy, V.Z. Pashkevych (2026). Research on a New Semiconductor Thermoelectric Material n-$Zr_{1-x}Nb_xNiSn$. I. Experimental Results. *Journal of Thermoelectricity*, (1), 5–16. https://doi.org/10.63527/1607-8829-2026-1-5-16

Received: 01.02.2026; Revised: 02.03.2026; Published: 31.03.2026

Introduction

Semiconductor solid solutions based on half-Heusler phases, in particular, n-TiNiSn, n-ZrNiSn, and n-HfNiSn, are among the most studied thermoelectric materials, since they have a high efficiency of converting thermal energy into electrical energy [1–4]. In semiconductor materials, to obtain maximum values of the thermoelectric figure of merit Z ($Z = \alpha^2 \cdot \sigma/\kappa$), the electric transport properties are optimized by appropriate doping, when the type of dopant and the conductivity of the semiconductor are the same [5–7].

In this context, the case where the optimization of electrokinetic properties is carried out by introducing Nb atoms ($4d^4 5s^1$) into the structure of the half-Heusler phase of n-ZrNiSn by substituting Zr atoms ($4d^2 5s^2$) in the 4*a* position, which generates structural defects of a donor nature (Nb has more *d*-electrons than Zr). Such doping of n-ZrNiSn the Fermi level ε_F (Fig. 1 *a*) closer to the level of the conduction band ε_C of n-$Zr_{1-x}Nb_xNiSn$, which corresponds to the condition for achieving maximum values of Z [5–7]. Considering that the atomic radius of Nb ($r_{Nb} = 0.1468$ nm) has an intermediate value between the corresponding values for Zr ($r_{Zr} = 0.1246$ nm) and Ni ($r_{Zr} = 0.1246$ nm) atoms, more complex transformations than linear substitution of Zr atoms by Nb are possible in the crystal structure of n-$Zr_{1-x}Nb_xNiSn$. Thus, studies of similar semiconductors n-$Ti_{1-x}Nb_xNiSn$ [8] and n-$Hf_{1-x}Nb_xNiSn$ [9] obtained by doping n-TiNiSn and n-HfNiSn with Nb atoms showed that Nb atoms can simultaneously occupy different crystallographic positions, generating structural defects of donor and acceptor nature. Therefore, one of the tasks of our study is to conduct a detailed analysis of structural transformations in n-$Zr_{1-x}Nb_xNiSn$.

Previous studies of the ZrNiSn half-Heusler phase have established several features of its crystal structure. It was shown that the structure of the ZrNiSn compound is disordered due to partial, up to ~ 1 %, occupation by Ni atoms ($3d^8 4s^2$) of the 4*a* position of Zr atoms ($4d^2 5s^2$), which generates structural defects of a donor nature (Ni has more *d*-electrons than Zr). At the same time, corresponding donor states are generated in the band gap ε_g, which fix the Fermi level ε_F (Fig. 1 *a*) and determine the electronic type of conductivity of n-ZrNiSn ("a priori doping" by donors [10]).

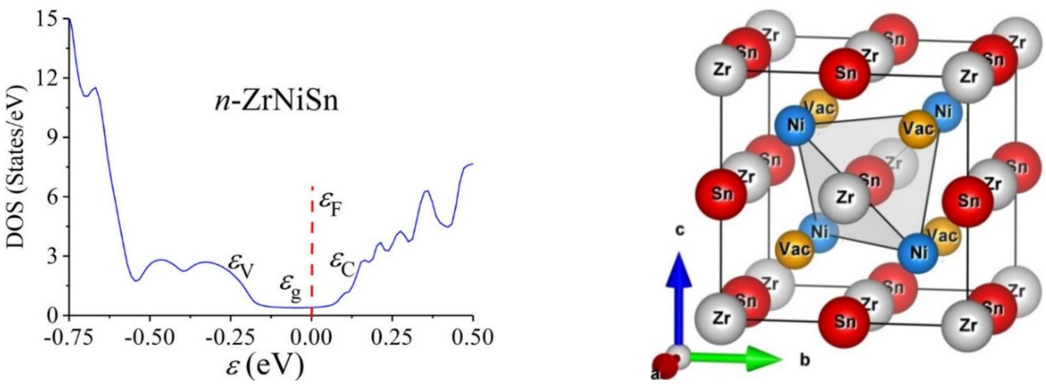

a *b*

Fig. 1. Distribution of the density of electronic states DOS (a) and model of the crystal structure (b) of the ZrNiSn compound [1]

Another feature of the ZrNiSn structure is the tetrahedral coordination of Ni atoms around Sn. The absence of a center of symmetry in the ZrNiSn compound is due to the presence of strong tetrahedral covalent bonds between atoms, which, on the one hand, is a guarantee of its semiconductor properties, and on the other hand, forms a volume in the unit cell that is ~ 24 % of the total, unoccupied by atoms (tetrahedral void). Tetrahedral voids can act as "traps" or vacancies (Vac) (Fig. 1 *b*) for both impurity atoms and compound atoms, generating structural defects of donor nature and corresponding energy states in the band gap ε_g [1].

Understanding the features of the crystal structure of the ZrNiSn half-Heusler phase is crucial to the successful analysis of structural studies of solid solutions based on it. On the other hand, knowledge of the features of the dynamics of the crystal structure of n-$Zr_{1-x}Nb_xNiSn$ will allow appropriate doping to generate energy states to obtain the maximum thermoelectric figure of merit *Z*. To determine the conditions for the synthesis of n-$Zr_{1-x}Nb_xNiSn$ with the maximum efficiency of converting thermal energy into electrical energy, it is necessary to establish the nature of the energy states and mechanisms of electrical conductivity, which is the subject of the study presented below.

Research methods

Experimental studies of the structural, kinetic, energy, and magnetic properties of the *n*-$Zr_{1-x}Nb_xNiSn$, $x = 0–0.07$, obtained by replacing Zr atoms in *n*-ZrNiSn with Nb atoms in position 4*a*, were carried out. $Zr_{1-x}Nb_xNiSn$ samples were obtained by electric arc-melting of the charge of the starting components in a purified argon atmosphere. To achieve an equilibrium state for the alloys, homogenizing annealing was performed at $T = 1073$ K for 700 h, followed by quenching in cold water without breaking the ampoules. *X*-ray phase analysis of the synthesized samples was performed by *X*-ray diffraction (PROTO AXRD Benchtop diffractometer (Cu K_α radiation). The elemental and chemical composition of the samples was controlled by energy-dispersive *X*-ray spectroscopy (Tescan Vega 3 LMU electron microscope). The structural parameters of the samples were calculated using the WinCSD program package [11]. For n-$Zr_{1-x}Nb_xNiSn$ samples, the temperature and concentration dependences of the electrical resistivity $\rho(T, x)$ and the thermopower coefficient $\alpha(T, x)$ were measured in the range T=80–400 K and the specific magnetic susceptibility $\chi(x)$ at $T = 300$ K. The thermopower coefficient $\alpha(T, x)$ was measured by the potentiometric method relative to copper. The voltage drop across the samples was measured accurately for different current directions to eliminate the influence of a potential p-n junction at the contact points.

Study of the features of the crystal structure of n-$Zr_{1-x}Nb_xNiSn$

Microprobe analysis of the chemical and phase compositions of the surface of the n-$Zr_{1-x}Nb_xNiSn$ samples, $x = 0–0.07$, established that it is the same and corresponds to the composition of the charge of the initial components. Fig. 2, as an example, shows a photograph of the surface along with the integral and elemental distribution of the components in the $Zr_{0.97}Nb_{0.03}NiSn$ sample.

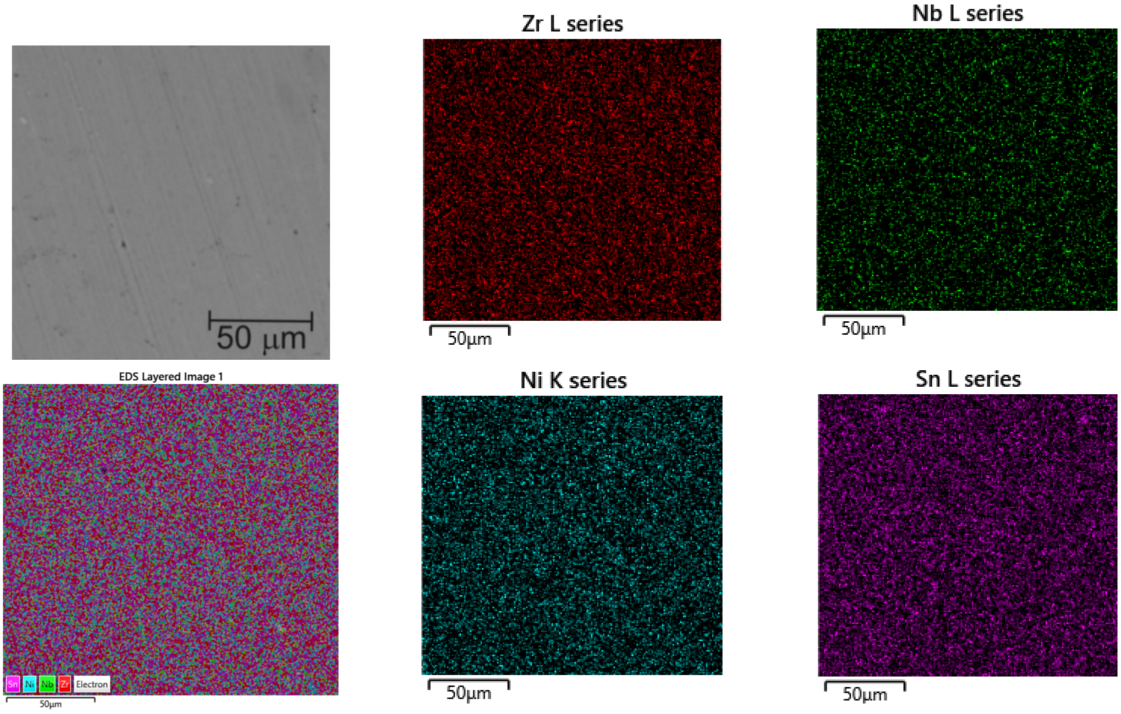

a *b*

Fig. 2. Surface photograph and integral (a) and elemental (b) distribution of the components in the $Zr_{0.97}Nb_{0.03}NiSn$ sample

In turn, *X*-ray structural studies have shown that the powder diffraction patterns of all n-$Zr_{1-x}Nb_xNiSn$ samples, $x = 0–0.05$, are indexed in the structure type MgAgAs (space group $F\bar{4}3m$) and there are no traces of other phases on them (Fig. 3*a*). In this case, Zr(Nb) atoms occupy the crystallographic position 4*a* (0, 0, 0), Ni – 4d (¼, ¼, ¼) and Sn – 4*c* (½, ½, ½). Our previous studies of the semiconductor solid solution $Zr_{1-x}Nb_xNiSn$ established the existence of solubility of Nb atoms up to a concentration of $x = 0.30$ inclusive [12]. However, the methods of *X*-ray analysis used at that time did not allow for identifying insignificant concentrations of foreign phases. The application of modern *X*-ray diffractometry and scanning electron microscopy has enabled the detection of negligible inclusions of the binary compound Nb_6Sn_5 in samples with concentrations *x* ranging from 0.07 to 0.15.

Based on experimental diffraction data, crystallographic parameters were calculated, in particular, inteatomic distances and the unit cell parameter $a(x)$ (Fig. 3*b*). Since the atomic radius of Nb (r_{Nb}=0.1468 nm) is smaller than that of Zr (r_{Zr}=0.1602 nm), a linear decrease in the unit cell parameter $a(x)$ was predicted, which should be adequate to the linear increase in the concentration of Nb atoms in the n-$Zr_{1-x}Nb_xNiSn$ solid solution samples. However, as shown in Fig. 3*b*, the decrease in the unit cell parameter $a(x)$ exhibits dependence close to linear only for the range $0 < x \leq 0.02$. It indicates the formation of a substitutional solid solution $Zr_{1-x}Nb_xNiSn$, where Nb atoms replace Zr atoms in position 4*a*. In this case, in n-$Zr_{1-x}Nb_xNiSn$, only structural defects of a donor nature are generated, and impurity donor states appear in the band gap ε_g, which determine electrical conductivity.

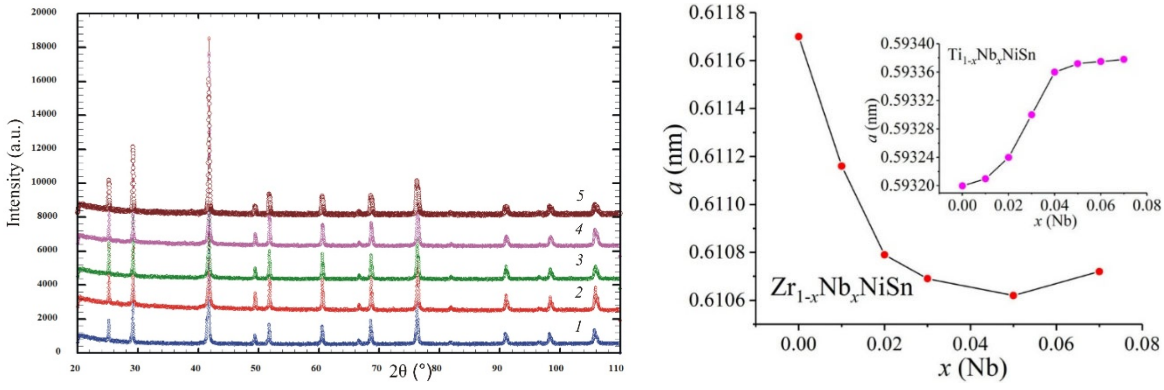

a *b*

Fig. 3. X-ray powder diffraction *patterns (1 – x = 0.01; 2 – x = 0.02; 3 – x = 0.03; 4 – x = 0.05; 5 – x = 0.07) (a) and change in the unit cell parameter a(x) (b) of $Zr_{1-x}Nb_xNiSn$ samples. Inset: change in the unit cell parameter a(x) of $Ti_{1-x}Nb_xNiSn$ [8]*

At higher concentrations of Nb atoms, $0.02 < x \leq 0.05$, the rate of change of the unit cell parameter $a(x)$ of n-$Zr_{1-x}Nb_xNiSn$ decreases significantly. Moreover, at concentrations of Nb atoms, $x > 0.05$, the unit cell parameter $a(x)$ unexpectedly increases (Fig. 3 *b*). This behavior of the dependence $a(x)$ for $x > 0.05$ does not correspond to the condition of the formation of a substitutional solid solution, when smaller Nb atoms replace larger Zr atoms. Considering that the change in the unit cell parameter of the solid solution is sensitive to the slightest alterations in the spatial arrangement of atoms, the behavior of $a(x)$ indicates more complex structural transformations in n-$Zr_{1-x}Nb_xNiSn$ than the substitution of Zr atoms for Nb atoms.

On the other hand, if the concentration of Nb atoms at $x = 0.05$ were the limit of the existence of a substitutional solid solution (the limit of solubility of Nb atoms in the semiconductor matrix), then the unit cell parameter $a(x)$ of n-$Zr_{1-x}Nb_xNiSn$ would not undergo significant changes. At the same time, the increase in the period $a(x)$ at $x > 0.05$ clearly indicates the existence of a semiconductor solid solution n-$Zr_{1-x}Nb_xNiSn$. Still, now the Nb atoms also simultaneously occupy other crystallographic positions.

Considering the peculiarities of the crystal structure of the half-Heusler phase ZrNiSn, the obtained experimental results of structural transformations in $Zr_{1-x}Nb_xNiSn$, where $x = 0$–0.07 can be explained consistently using the two models of the ZrNiSn compound described above. Thus, if in $Zr_{1-x}Nb_xNiSn$ in the crystallographic position 4 *a*, Zr atoms ($r_{Zr} = 0.1602$ nm) are replaced by Nb atoms ($r_{Nb} = 0.1468$ nm), then the decrease in the unit cell parameter $a(x)$ within the concentrations $0 < x \leq 0.02$ according to a linear law is logical. In turn, the reduction in the rate of change of the unit cell parameter $a(x)$ of $Zr_{1-x}Nb_xNiSn$ at concentrations $0.02 < x \leq 0.05$ can be associated with the simultaneous partial substitution of Zr atoms by Nb atoms and the occupation of tetrahedral voids of the structure by Nb atoms. Thus, if the substitution of Zr atoms by Nb atoms leads to a decrease in the unit cell parameter $a(x)$ of $Zr_{1-x}Nb_xNiSn$, then the occupation of tetrahedral voids of the structure (“traps” or vacancies (Vac) [1]) by Nb atoms leads to an increase in the unit cell parameter $a(x)$. It is what “slows down” the integral decrease in the unit cell parameter $a(x)$ of $Zr_{1-x}Nb_xNiSn$. In this case, in $Zr_{1-x}Nb_xNiSn$, two types of structural defects of donor nature and the corresponding energy states in the band gap ε_g are simultaneously generated in different ratios. At the same time, the increase in the unit cell parameter $a(x)$ of $Zr_{1-x}Nb_xNiSn$ for $x > 0.05$ clearly indicates the preferential occupation of tetrahedral voids of the structure by Nb atoms and the generation of donors.

On the other hand, if we take as a basis the disordered model of the crystal structure of the half-Heusler phase ZrNiSn, in which Ni atoms are existent at position 4*a* [10], then we can assume that the decrease in the rate of change of the unit cell parameter $a(x)$ at $x = 0.03–0.05$ is the result of the preferential substitution of Zr atoms by Nb atoms at position 4*a* and the simultaneous partial substitution of Ni atoms present there ($r_{Ni} = 0.125$nm). At the same time, the increase in the unit cell parameter $a(x)$ of $Zr_{1-x}Nb_xNiSn$ at $x > 0.05$ is possible only with the preferential displacement of Ni atoms ($4d^45s^1$) availeble at position 4*a* by Nb atoms ($4d^45s^1$). In this case, structural defects of an acceptor nature and the corresponding acceptor states are generated in n-$Zr_{1-x}Nb_xNiSn$ (Nb has fewer *d*-electrons than Ni). It should lead to an increase in the compensation degree of n-$Zr_{1-x}Nb_xNiSn$, which indicates the ratio of ionized donor and acceptor states [13]. The results of the electrokinetic, energetic, and magnetic properties of $Zr_{1-x}Nb_xNiSn$ presented below will clarify the previous conclusions of the structural studies.

Electrokinetic, energetic and magnetic properties of n-$Zr_{1-x}Nb_xNiSn$

Fig. 4 shows the temperature dependences of the electrical resistivity $\rho(T, x)$ and the thermopower coefficient $\alpha(T, x)$ of n-$Zr_{1-x}Nb_xNiSn$, $x = 0.01–0.07$. As seen that even at the lowest concentration of Nb atoms, $x = 0.01$, the resistivity $\rho(T, x)$ of n-$Zr_{1-x}Nb_xNiSn$, which in n-ZrNiSn decreased exponentially [10], monotonically increases with temperature (Fig. 4*a*). Metallization of electrical conductivity occurred when the Fermi level ε_F, which in n-ZrNiSn was in the band gap ε_g near the conduction band ε_C (Fig. 1*a*), was now located in the band of continuous energies: a dielectric-metal conduction transition occurred [13, 14]. The location of the Fermi level ε_F precisely in the conduction band is indicated by the negative values of the thermopower coefficient $\alpha(T, x)$ at all temperatures (Fig. 4*b*), and the action of the current carrier scattering mechanisms is the cause of the increase in the resistivity $\rho(T, x)$ with temperature.

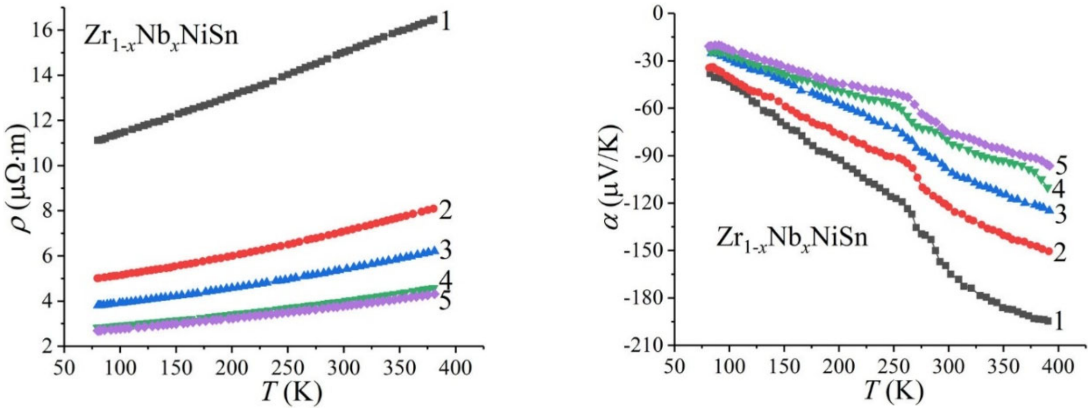

a *b*

Fig. 4. Temperature dependences of the resistivity $\rho(T, x)$ (a) and the thermopower coefficient $\alpha(T, x)$ (b) of n-$Zr_{1-x}Nb_xNiSn$: 1 – $x = 0.01$; 2 – $x = 0.02$; 3 – $x = 0.03$; 4 – $x = 0.05$; 5 – $x = 0.07$

A priori, we sought to obtain a series of n-$Zr_{1-x}Nb_xNiSn$ samples with concentrations at which the Fermi level ε_F consistently approaches the conduction band ε_C, facilitating the thermal injection of electrons from donor states into the conduction band ε_C. Such dynamics of the Fermi level ε_F corresponded to the condition for achieving maximum efficiency of thermal energy conversion into electrical energy [5–7]. However, already at the Nb concentration of $x = 0.01$, a sufficient number of donor states was generated for the Fermi level ε_F in n-$Zr_{0.99}Nb_{0.01}NiSn$ to enter the conduction band ε_C. It is clear that at all subsequent concentrations of n-$Zr_{1-x}Nb_xNiSn$, $0.01 < x \leq 0.07$, the behavior of the temperature dependences $\rho(T, x)$ and $\alpha(T, x)$ is similar (Fig. 4).

The behavior of the resistivity $\rho(x, T)$ and the thermopower coefficient $\alpha(x, T)$ of n-$Zr_{1-x}Nb_xNiSn$ when the concentration of Nb atoms changes at different temperatures is interesting and informative (Fig. 5). As seen from Fig. 5*a*, the resistivity $\rho(x, T)$ of n-$Zr_{1-x}Nb_xNiSn$ decreases at all studied temperatures with an increase in the concentration of Nb atoms. This behavior of $\rho(x, T)$ is due to the rise in the concentration of donors and free electrons in n-$Zr_{1-x}Nb_xNiSn$ during their ionization.

We draw attention to the different order of the dependences $\rho(x, T)$ at concentrations $0 \leq x < 0.01$ and $0.01 \leq x \leq 0.07$. Thus, at concentrations $0 \leq x < 0.01$, the higher the temperature, the lower the electrical resistivity and the dependence $\rho(x, T)$ at the highest temperature $T = 380$ K is located lowest in Fig. 5*a*. This behavior of the electrical resistivity $\rho(x, T)$ n-$Zr_{1-x}Nb_xNiSn$ is due to the increase in the concentration of free electrons during their thermal activation from the Fermi level ε_F, fixed by donor states in the band gap ε_g, to the conduction band ε_C. At the same time, the higher the temperature, the greater the number of electrons will pass into the conduction band. At the same time, at concentrations $0.01 \leq x \leq 0.07$, when the Fermi level ε_F is already in the band of continuous energies, an increase in temperature leads to an increase in the probability of electron scattering. The higher the temperature, the greater the electrical resistivity, and the dependence $\rho(x, T)$ for $T = 380$ K is located highest in Fig. 5*a*.

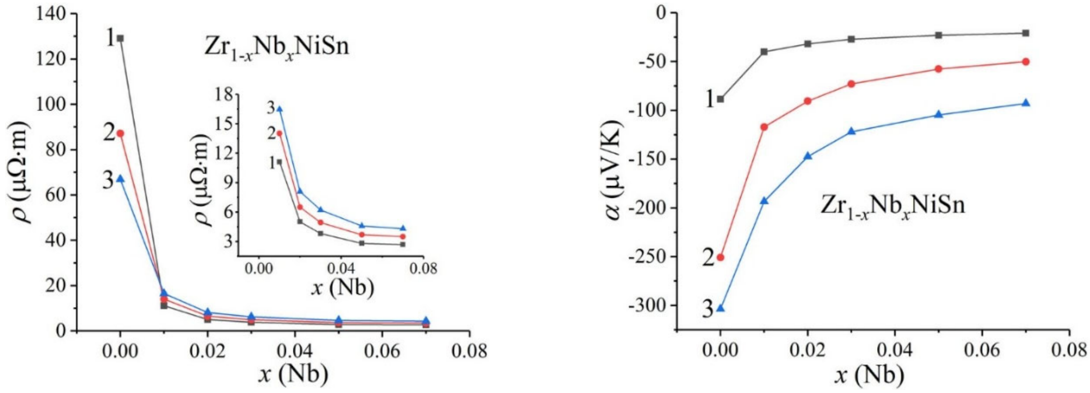

a *b*

Fig. 5. Change in resistivity ρ(x, T) (a) and thermopower coefficient α(x, T) (b) of $Zr_{1-x}Nb_xNiSn$ at different temperatures: 1 – T=80 K; 2 – T=250 K; 3 – T=380 K

Analysis of the temperature (Fig. 4) and concentration (Fig. 5) dependences of the resistivity ρ and the thermopower coefficient *α* of n-$Zr_{1-x}Nb_xNiSn$, $x = 0.01$–0.07, did not reveal the effects of acceptor states that could be generated in the case of partial substitution of Ni atoms by Nb atoms. This experimental result confirms the structural model, which assumes simultaneous partial substitution of Zr atoms by Nb atoms and occupation of the tetrahedral voids of the structure by Nb atoms. Such transformations in the n-$Zr_{1-x}Nb_xNiSn$ structure are accompanied by the generation of only donors and the corresponding energy states.

Another proof that n-$Zr_{1-x}Nb_xNiSn$ does not generate acceptor states is the behavior of the activation energy ε_1^{α}, determined from the high-temperature parts of the thermopower coefficient $\alpha(1/T)$. The fact is that n-$Zr_{1-x}Nb_xNiSn$ a priori contains a large number of structural defects and is a heavily doped and compensated semiconductor (HDCS) [13]. The presence in a semiconductor of a significant number of different charged defects, the location of which is of a fluctuating nature, radically changes its electronic structure and leads to fluctuations in the potential relief and modulation of continuous energy bands [13].

The authors [1] showed that the numerical values of the activation energy $\varepsilon_1^{\alpha}(x)$, derived from the activation parts of the temperature dependences of the thermopower coefficient $\alpha(1/T)$, are proportional to the amplitude of the modulation of the continuous energy bands of the HDCS. In turn, the amplitude of the large-scale fluctuation of the continuous energy bands is proportional to the compensation degree of the semiconductor: a higher compensation degree results in a greater amplitude of band modulation. Fig. 6*a* shows the temperature dependences of the thermopower coefficient $\alpha(1/T, x)$ for n-$Zr_{1-x}Nb_xNiSn$, which can be described using the well-known formula [14]:

$$\alpha = \frac{k_B}{e}\left(\frac{\varepsilon_i{}^{\alpha}}{k_B T} - \gamma + 1\right),$$

where γ is a parameter that depends on the nature of the scattering mechanisms. From the high-temperature activation parts of the $\alpha(1/T, x)$ dependences of n-$Zr_{1-x}Nb_xNiSn$ (Fig. 6*a*), the activation energies $\varepsilon_1^{\alpha}(x)$ (Fig. 6*b*) were calculated, which are proportional to the amplitude of the large-scale fluctuation of the continuous energy bands of the HDCS [1, 13].

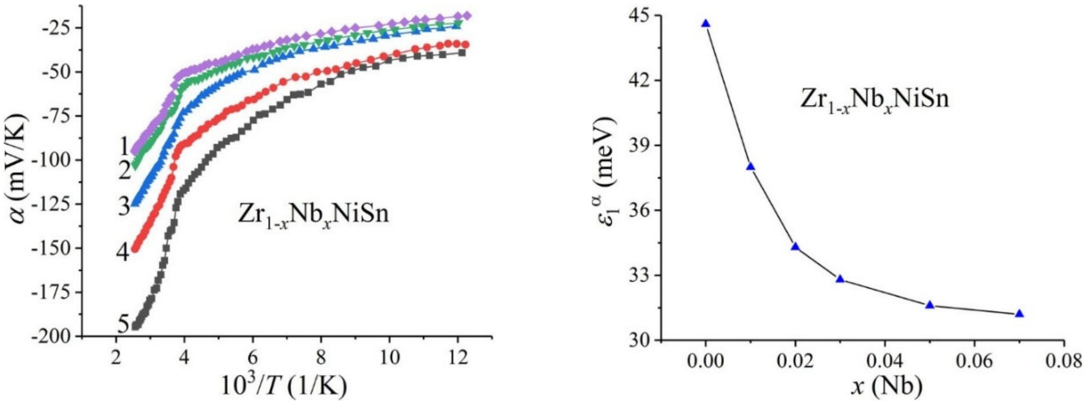

a *b*

Fig. 6. Temperature dependences of the thermopower coefficient $\alpha(1/T)$ (a) and the change in activation energy $\varepsilon_1^{\alpha}(x)$ (b) of $Zr_{1-x}Nb_xNiSn$. a: 1 – $x = 0.07$; 2 – $x = 0.05$; 3 – $x = 0.03$; 4 – $x = 0.02$; 5 – $x = 0.01$

From the results shown in Fig. 6*b*, it follows that with increasing concentration of Nb atoms, the activation energy $\varepsilon_1^{\alpha}(x)$ decreases. Thus, if in n-ZrNiSn the activation energy was

$\varepsilon_1^{\alpha}{}_{(x=0)} = 44.6$ meV, then in the semiconductor n-$Zr_{0.99}Nb_{0.01}NiSn$ it decreased to $\varepsilon_1^{\alpha}{}_{(x=0.01)} = 38.1$ meV and to $\varepsilon_1^{\alpha}{}_{(x=0.07)} = 31.2$ meV in n-$Zr_{0.93}Nb_{0.07}NiSn$. The decrease in the activation energy $\varepsilon_1^{\alpha}(x)$ indicates a decrease in the amplitude of modulation of continuous energy bands, which in the semiconductor of the electronic conduction type n-$Zr_{1-x}Nb_xNiSn$ is possible only if it is doped with donors [13]. Another experimental confirmation was obtained that only defects of donor nature and corresponding energy states are generated in n-$Zr_{1-x}Nb_xNiSn$. It is realized in the case of simultaneous partial substitution of Zr atoms by Nb atoms, along with occupation of tetrahedral voids by Nb atoms.

Experimental measurements of the specific magnetic susceptibility $\chi(x)$ of n-$Zr_{1-x}Nb_xNiSn$ samples at room temperature showed that the based semiconductor compound n-ZrNiSn is a weak diamagnet, which is reflected by the negative values of the magnetic susceptibility ($\chi = -0.07 \cdot 10^{-6}$ emu/g) (Fig. 7*a*). However, even at a low concentration of Nb atoms, the n-$Zr_{1-x}Nb_xNiSn$ semiconductor becomes a Pauli paramagnet with its inherent small values of the specific magnetic susceptibility ($\chi \sim 10^{-6}$ emu/g). It is known that in Pauli paramagnets the magnetic susceptibility is determined by free electrons and is proportional to the density of electronic states at the Fermi level $g(\varepsilon_F)$. As seen from Fig. 7*a*, in the paramagnetic region, an increase in the concentration of Nb atoms leads to an increase in the specific magnetic susceptibility $\chi(x)$ for n-$Zr_{1-x}Nb_xNiSn$. It means that the concentration of free electrons increases in the semiconductor during the ionization of donor states, which is possible only with an increase in their concentration. Thus, an increase in the concentration of donor states has been established experimentally, which may be the result of the simultaneous partial substitution of Zr atoms by Nb atoms and the occupation of the tetrahedral voids of the structure by Nb atoms.

The results of electrokinetic studies allowed us to obtain a change in the thermoelectric power factor $Z^*(x)$ of n-$Zr_{1-x}Nb_xNiSn$ with concentration at $T = 300$ K (Fig. 7*b*). It is evident from Fig. 7*b* that at the concentration of Nb atoms, $x \approx 0.04$, the dependence $Z^*(x)$ reaches a maximum, which indicates the highest efficiency of converting thermal energy into electrical energy. The obtained results of experimental studies show that the n-$Zr_{1-x}Nb_xNiSn$ semiconductor substitutional solid solution is a promising thermoelectric material.

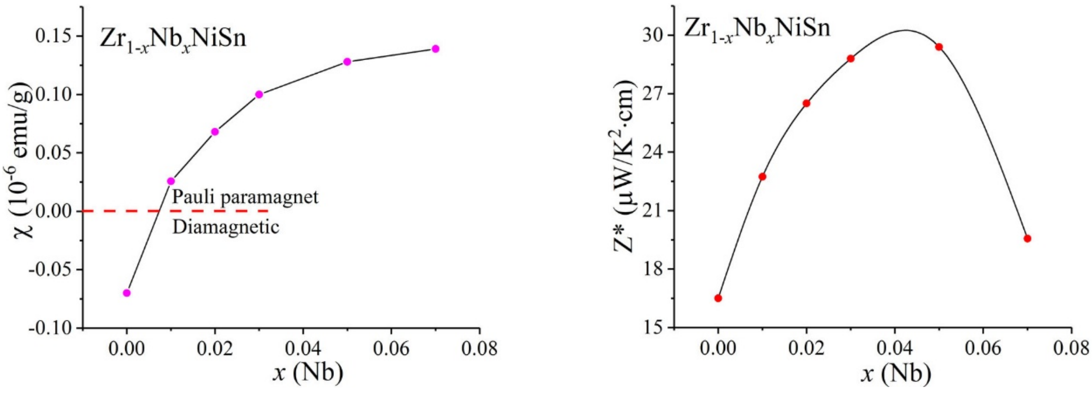

a *b*

Fig. 7. Change in specific magnetic susceptibility $\chi(x)$ (a) and thermoelectric power factor $Z^*(x)$ (b) of $Zr_{1-x}Nb_xNiSn$

Thus, experimental measurements of the properties of the semiconductor solid solution n-$Zr_{1-x}Nb_xNiSn$, $x = 0–0.07$, have established that at all Nb concentrations in the semiconductor, only defects of donor nature and the corresponding energy states are generated. It corresponds to the condition for obtaining maximum values of the thermoelectric figure of merit [5–7]. Modeling the properties of n-$Zr_{1-x}Nb_xNiSn$ will be the next stage of the study, which will be used to determine the optimal conditions for synthesizing a thermoelectric material with maximum efficiency of converting thermal energy into electrical energy.

Conclusions

The structural, electrokinetic, energetic, and magnetic properties of the new semiconductor thermoelectric material n-$Zr_{1-x}Nb_xNiSn$, $x = 0–0.07$, obtained by doping n-ZrNiSn with Nb atoms ($4d^45s^1$) by replacing Zr atoms ($4d^25s^2$) have been investigated. The nature of the generated energy states and mechanisms of electrical conductivity have been established. It has been shown that in the n-$Zr_{1-x}Nb_xNiSn$ structure, there is a simultaneous substitution of Zr atoms by Nb atoms in different ratios, as well as the occupation of tetrahedral voids of the structure by Nb atoms. The decrease in the unit cell parameter $a(x)$ of n-$Zr_{1-x}Nb_xNiSn$ samples at concentrations $0 < x \leq 0.05$ is caused by the preferential partial substitution of Zr atoms ($r_{Zr} = 0.1602$ nm) by Nb atoms ($r_{Nb} = 0.1468$ nm) and the increase in the unit cell parameter $a(x)$ at $0.05 < x$ is caused by the preferential occupation of tetrahedral voids by Nb atoms. Structural transformations of n-$Zr_{1-x}Nb_xNiSn$ generate two types of defects of donor nature and the corresponding energy states of the band gap ε_g, which meet the condition for obtaining the maximum efficiency of converting thermal energy into electrical energy. It is shown that the n-$Zr_{1-x}Nb_xNiSn$ semiconductor substitutional solid solution is a promising thermoelectric material.

Acknowledgements

The work was carried out within the framework of grants of the Ministry of Education and Science of Ukraine No. 0124U000989 and No. 0124U001146. The authors Stadnyk Yu.V., Romaka L.P., Horyn A.M. and Zelinsky A.V. are grateful for the financial support of the Simons Foundation (SFI-PD-Ukraine-00014574).

Authors' information

V.A. Romaka – D.Sc., Professor.
Yu.V. Stadnyk – Ph.D., Senior Scientist.
L.P. Romaka – Ph.D., Senior Scientist.
A.M. Horyn – Ph.D., Senior Scientist.
A.V. Zelinskiy – Ph.D., Senior Scientist.
V.Z. Pashkevych – D.Sc., Professor.

References

1. Romaka V.A., Pashkevych V.Z., Romaka L.P., Stadnyk Yu.V., Romaka V.V., Kovtun S.I., Horyn A.M. (2025). *New thermoelectric materials based on half-Husler phases*. Publishing House of Lviv Polytechnic National University, 628 p. DOI: https://ena.lpnu.ua/handle/ntb/111829.
2. Arachchige V.G., Recalcati S., Rossa J., Yoon S., Skokov K., Radulov I., Klemenz S. (2025). Thermoelectric properties of electro-sinter forged ZrNiSn. *J. Alloys Compd.* 1045, 184694. https://doi.org/10.1016/j.jallcom.2025.184694
3. Berry T., Fu Ch., Auffermann G., Fecher G.H., Schnelle W., Serrano-Sanchez F., Yue Y., Liang H., Felser C. (2017). Enhancing thermoelectric performance of TiNiSn half-Heusler compounds via modulation doping. *Chem Mater.* 29 (16), 7042-7048. https://doi.org/10.1021/acs.chemmater.7b02685
4. Du N.V., Nam W.H., Cho J.Y., Binh N.V., Huy P.T., Trung D.Q., Tuan D.A., Shin W.H., Lee S. (2021). Enhanced thermoelectric properties of Hf-free half-Heusler compounds prepared via highly fast process. *J. Alloys Compd.* 886, 161293. https://doi.org/10.1016/j.jallcom.2021.161293.
5. Anatychuk L.I. (1998). *Thermoelectricity*. Physics of thermoelectricity, Institute of Thermoelectricity, Kyiv, Chernivtsi, Vol. 1, 376 p.
6. Romaka V.A., Fruchart D., Stadnyk Yu.V., Tobola J., Gorelenko Yu.K., Shelyapina M.G., Romaka L.P., Chekurin V.F. (2006). Conditions for attaining the maximum values of thermoelectric power in intermetallic semiconductors of the MgAgAs structural type. *Semiconductors*, 40 (11), 1275–1281. DOI: https://doi.org/10.1134/S1063782606110054.
7. Romaka V.A., Rogl P., Stadnyk Yu.V., Hlil E.K., Romaka V.V., Horyn A.M. (2012). Features of Conductivity of the Intermetallic Semiconductor *n*-ZrNiSn Heavily Doped with a Bi Donor Impurity. *Semiconductors,* 46 (7), 887–893.
   DOI: 10.1134/S1063782612070172.
8. Romaka V.A., Stadnyk Yu.V., Romaka L.P., Horyn A.M., Romaka V.V., Haraniuk P.I. (2025). Research of Thermoelectric Material $Ti_{1-x}Nb_xNiSn$. *Journal of Thermoelectricity*, №1, 5–15.
   DOI: 10.63527/1607-8829-2025-1-5-15.
9. Romaka L., Stadnyk Yu., Romaka V.A., Horyn A., Romaka V.V., Demchenko P., Haranyuk P. (2025). Research on a new thermoelectric material obtained by doping of *n*-HfNiSn with Nb atoms. *Physics and Chemistry of Solid State*, 26 (4), 787–793. DOI: 10.15330/pcss.26.4.787-793.
10. Romaka V.A., Stadnyk Yu.V., Romaka V.V., Fruchart D., Gorelenko Yu.K., Chekurin V.F., Goryn A.M. (2007). Features of electrical conductivity in the *n*-ZrNiSn intermetallic semiconductor heavily doped with the In acceptor impurity. *Semiconductors,* 41 (9), 1041–1047. DOI: 10.1134/S1063782607090072.
11. Akselrud L., Grin Yu. (2014). WinCSD: software package for crystallographic calculations (Version 4). *J. Appl. Crystallogr.*, 47, 803–805.
    DOI: https://doi.org/10.1107/S1600576714001058.

12. Stadnyk Yu.V., Romaka L.P., Goryn A.M., Tatomyr Ya.T., Skolozdra R.V. (1997). Electrophisical and magnetic properties of solid solutions $Zr_{1-x}Nb_xNiSn$ and $Zr_{1-x}Mo_xNiSn$. *Journal of Thermoelectricity*, №1, 56–61.
13. Shklovskii B.I. and Efros A.L. (1984). *Electronic properties of doped semiconductors*. Berlin, Heidelberg, NY, Tokyo, Springer-Verlag, 388 p. DOI: 10.1007/978-3-662-02403-4.
14. Mott N.F. and Davis E.A. (2012). *Electron processes in non-crystalline materials*. Oxford, Clarendon Press, 590 p. DOI: https://doi.org/10.1002/crat.19720070420.

Романа В.А.[1] (https://orcid.org/0000-0002-2984-9513),
Стадник Ю.В.[2] (https://orcid.org/0000-0003-0692-2973),
Ромака Л.П.[2] (https://orcid.org/0000-0001-5793-4435),
Горинь А.М.[2] (https://orcid.org/0000-0003-3483-8808),
Зелінський А.В.[2] (https://orcid.org/0000-0001-8473-1174),
Пашкевич В.З.[1] (https://orcid.org/0000-0002-6849-652X)

[1]Національний університет "Львівська політехніка",
вул. С. Бандери, 12, Львів, 79013, Україна;
[2]Львівський національний університет ім. І. Франка,
вул. Кирила і Мефодія, 6, Львів, 79005, Україна

Дослідження нового напівпровідникового термоелектричного матеріалу n-$Zr_{1-x}Nb_xNiSn$. I. Результати експерименту

Досліджено структурні, електрокінетичні, енергетичні та магнітні властивості нового напівпровідникового термоелектричного матеріалу n-$Zr_{1-x}Nb_xNiSn$, $x = 0$–0.07, отриманого легуванням n-ZrNiSn атомами Nb ($4d^45s^1$) шляхом заміщення атомів Zr ($4d^25s^2$). Встановлено природу генерованих енергетичних станів та механізмів електропровідності. Показано, що в структурі n-$Zr_{1-x}Nb_xNiSn$ відбувається одночасне заміщення у різних співвідношеннях атомів Zr на атоми Nb, а також зайняття атомами Nb тетраедричних пустот структури. Зменшення періоду комірки a(x) n-$Zr_{1-x}Nb_xNiSn$ за концентрацій $0 < x \leq 0.05$ викликане переважним частковим заміщення атомів Zr ($r_{Zr} = 0.1602$ нм) на атоми Nb ($r_{Nb} = 0.1468$ нм), а збільшення періоду a(x) за $0.05 < x$ – переважним зайняттям атомами Nb тетраедричних пустот структури. Структурні перетворення n-$Zr_{1-x}Nb_xNiSn$ генерують два сорти дефектів донорної природи та відповідні енергетичні стани забороненої зони ε_g, що відповідає умові отримання максимальної ефективності перетворення теплової енергії в електричну. Показано, що напівпровідник n-$Zr_{1-x}Nb_xNiSn$ є перспективним термоелектричним матеріалом.

Ключові слова: термоелектричний матеріал, напівпровідник, електронна структура, електроопір, коефіцієнт термо-ерс, термоелектрична добротність.